Chapter

Thermal Fields in Laser Cladding Processing: A "Fire Ball" Model. A Theoretical Computational Comparison, Laser Cladding versus Electron Beam Cladding

Mihai Oane, Ion N. Mihăilescu and Carmen-Georgeta Ristoscu

Abstract

Laser cladding processing can be found in many industrial applications. A lot of different materials processing were studied in the last years. To improve the process, one may evaluate the phenomena behaviour from a theoretical and computational point of view. In our model, we consider that the phase transition to the melted pool is treated using an absorption coefficient which can underline liquid formation. In the present study, we propose a semi-analytical model. It supposes that melted pool is in first approximation a "sphere", and in consequence, the heat equation is solved in spherical coordinates. Using the Laplace transform, we will solve the heat equation without the assumption that "time" parameter should be interpolated linearly. 3D thermal graphics of the Cu substrate are presented. Our model could be applied also for electron cladding of metals. We make as well a comparison of the cladding method using laser or electron beams. We study the process for different input powers and various beam velocities. The results proved to be in good agreement with data from literature.

Keywords: laser cladding, electron beam cladding, heat equation, computer simulations

1. Introduction

The laser processing of materials is a continuous subject of study from a practical and theoretical point of view [1–3]. Laser cladding is a very important application in laser processing [4]. Laser cladding started in the 1980s and was widely implemented in industry. Meanwhile, the application of the laser cladding has exploded especially in 3D additive manufacturing at a relatively low production cost. From theoretical point of view, the mentioned application was studied in Refs. [5, 6]. In the present study, we want to generalize the existent theory to laser beams with different transverse multimode intensities. We will use the heat diffusion equation for the melted pool [5, 6]. We note the depth of the melted pool with H. It is reasonable to consider that the depth of the melted pool varies between 0.2 and 2.5 mm, for a CO_2 incident laser beam of 1 KW. The speed of laser is considered to

vary from 0 to 100 mm/s. The main purpose of engineering technology science is to achieve the best quality of the product with the maximum use of facilities and resources. In these terms, laser cladding is a very delicate process. In consequence, all kinds of modelling are welcome. In general, we find in literature a lot of experiments, but for a laboratory which wants to start to build up a laser cladding set-up for the first time, theoretical and computer modelling are essential for the experimental success.

The powder attenuation is defined as the following ratio:

$$X_p = \frac{P_L - P'_L}{P_L} \tag{1}$$

where P_L is the laser power and P'_L is the transmitted laser power, which is in interaction with the work piece surface. We will focus to determine the temperature in the melted pool. For this we will choose a more realistic model (regarding the "time" parameter), writing the heat carried into the melted pool by the expression:

$$Q_P = I(X,Y,Z) \cdot (\alpha_P X_P + \alpha_P X_P (1-\alpha_P)(1-\alpha_W)(h(t) - h(t-t_0)) = Q_P\,(r,\theta,\varphi) \tag{2}$$

where t_0 is the exposure time, α_P is powder absorption coefficient and α_W is the workpiece absorption coefficient.

2. The analytical model

The novelty of the proposed model is that we consider the melted pool like a sphere with diameter H. Using the Laplace transform, we will solve the heat equation avoiding making the assumption that "time" parameter should be interpolated linearly. The heat equation in spherical coordinates is:

$$\frac{\partial^2 T}{\partial r^2} + \frac{2}{r}\frac{\partial T}{\partial r} + \frac{1}{r^2}\left[\frac{\partial}{\partial \mu}\left(1-\mu^2\right)\frac{\partial T}{\partial \mu}\right] + \frac{1}{r^2}\cdot\frac{1}{(1-\mu^2)}\frac{\partial^2 T}{\partial \varphi^2} = \frac{1}{\gamma}\frac{\partial T}{\partial t} - \frac{Q_P(r,\theta,\varphi,t)}{k} \tag{3}$$

In Eq. (3), T is temperature variation; r, θ and φ are the spherical coordinates; γ is thermal diffusivity; and k represents the thermal conductivity. For simplicity, we will note for the rest of the present study $Q = Q_P$.

We have the following relationships:

$$T|_{t=0} = 0 \text{ and } \mu = \cos\theta \tag{4}$$

The boundary conditions are:

$$k\frac{\partial T}{\partial r}\bigg|_{r=a} + h \cdot T = 0 \tag{5}$$

where $a = H/2$ is the irradiated sphere radius and h is the thermal transfer coefficient.

We have the following relationships that are necessary to eliminate the variable φ:

$$\frac{\partial^2 F_1}{\partial \varphi^2} + m^2 F_1 = 0 \text{ and } F_1|_{\varphi=0} = F_1|_{\varphi=2\pi} \tag{6}$$

We obtain:

$$F_1(\varphi) = \cos m\varphi \text{ for } p = 2m \tag{7}$$

and

$$F_2(\varphi) = \sin m\varphi \text{ for } p = 2m - 1 \tag{8}$$

Such conditions lead to:

$$\frac{\partial^2 \overline{T}}{\partial r^2} + \frac{2}{r}\frac{\partial \overline{T}}{\partial r} + \frac{1}{r^2}\left\{\frac{\partial}{\partial \mu}\left(1-\mu^2\right)\frac{\partial \overline{T}}{\partial \mu} - \frac{m^2}{1-\mu^2}\overline{T}\right\} = \frac{1}{\gamma}\frac{\partial \overline{T}}{\partial t} - \frac{\overline{Q(r,\theta,p,t)}}{k} \tag{9}$$

where

$$\overline{T}(r,\theta,p,t) = \overline{T}(r,\theta,m,t) = \int_0^{2\pi} T\,(r,\theta,\varphi,t) F_{1p}(\varphi)\, d\varphi; p = \begin{cases} 2m \\ 2m-1 \end{cases} \tag{10}$$

Now, in order to eliminate the variable θ, we assume that:

$$F_3\overline{T} = \frac{\partial}{\partial \mu}\left[\left(1-\mu^2\right)\frac{\partial \overline{T}}{\partial \mu}\right] - \frac{m^2}{1-\mu^2}\overline{T} \tag{11}$$

We have:

$$\frac{\partial}{\partial \mu}\left[\left(1-\mu^2\right)\frac{\partial F_3}{\partial \mu}\right] + \left(\lambda - \frac{m^2}{1-\mu^2}\right)F_3 = 0 \tag{12}$$

where

$$\lambda = n(n+1)(n = 0,1,2,3....) \text{ and } F_3 = P_{nm}(\cos(\theta)) \tag{13}$$

where P_{nm} are the associated Legendre polynomials.
To eliminate the variable r, we have to consider that:

$$\frac{\partial^2 \widetilde{T}}{\partial r^2} + \frac{2}{r}\frac{\partial \widetilde{T}}{\partial r} - \frac{n(n+1)}{r^2}\widetilde{T} = \frac{1}{k}\frac{\partial \widetilde{T}}{\partial t} - \widetilde{Q}\,(r,\gamma,p,t) \tag{14}$$

where $\gamma = \begin{cases} 2m \\ 2m-1 \end{cases}$ and the heat equation is the following:

$$\widetilde{T} = \frac{\widetilde{v}}{r^{1/2}}\frac{\partial^2 \widetilde{v}}{\partial r^2} + \frac{1}{r}\frac{\partial \widetilde{v}}{\partial r} - \frac{\left(n+\frac{1}{2}\right)^2}{r^2}\widetilde{v} = \frac{1}{\gamma}\frac{\partial \widetilde{v}}{\partial t} - \widetilde{Q}(r,\gamma,p,t) \tag{15}$$

We have:

$$\frac{\partial^2 F_3}{\partial r^2} + \frac{1}{r}\frac{\partial F_3}{\partial r} + \left[\lambda^2 - \frac{\left(n+\frac{1}{2}\right)^2}{r}\right]F_3 = 0 \tag{16}$$

The theory says that:

$$|F_3||_{r=0} < \infty \; si \; k\left.\frac{\partial F_3}{\partial r}\right|_{r=a} + hF_3 = 0 \tag{17}$$

The obtained result is:

$$F_3 = J_{n+\frac{1}{2}}(\lambda a) \tag{18}$$

and

$$k\left(J_{n-\frac{1}{2}}(\lambda_{ns}a) - J_{n+\frac{1}{2}}(\lambda_{ns}a)\right) + hJ_{n+\frac{1}{2}}(\lambda_{ns}a) = 0 \tag{19}$$

To eliminate the temporal variable, we use the direct and reverse Laplace transform. Thus we obtain [1]:

$$\begin{aligned} T(r,\theta,\varphi,t) = {} & \frac{1}{r^{\frac{1}{2}}}\sum_{m=0}^{\infty}\sum_{n,\,s=1}^{\infty}\frac{1}{C_{mn}\cdot C_{ns}}\cdot\frac{1}{\lambda_{ns}^2}\left[1-e^{-\lambda_{ns}^2 t}-\left(1-e^{-\lambda_{ns}^2\cdot(t-t_0)}\right)\cdot H(t-t_0)\right] \\ & \cdot J_{n+\frac{1}{2}}(\lambda_{ns}r)\left[P_{n\,m}(\cos\theta)\cos(m\varphi)\cdot\left(\int_0^a\int_0^{2\pi}\int_0^{\theta_{max}}\cdot\frac{E(E_0,r,\cos\theta)}{C}\cdot r^{\frac{3}{2}}\cdot J_{n+\frac{1}{2}}(\lambda_{ns}r)\right.\right. \\ & \left.\left.\cdot P_{n\,m}(\cos\theta)\cdot\cos(m\varphi)drd\theta d\varphi\right)+P_{n\,m}(\cos\theta)\cdot\sin(m\varphi)\right. \\ & \left.\cdot\left(\int_0^a\int_0^{2\pi}\int_0^{\theta_{max}}\cdot\frac{E(E_0,r,\cos\theta)}{C}\cdot r^{\frac{3}{2}}\cdot J_{n+\frac{1}{2}}(\lambda_{ns}r)\cdot P_{n\,m}(\cos\theta)\cdot\sin(m\varphi)drd\theta d\varphi\right)\right] \end{aligned} \tag{20}$$

In the above relationship:

$$C_{m\,n} = \int_{-1}^{+1}[P_{m\,n}(\mu)]^2\,d\mu = \frac{2\delta}{2}\frac{(n+m)!}{n+1\,(n-m)!} \tag{21}$$

and

$$\delta = \begin{cases} 2 for\ m = 0 \\ 1 for\ m \neq 0 \end{cases} \tag{22}$$

but also

$$C_{ns} = \frac{1}{2}\,a\left[J'_{n+\frac{1}{2}}(\lambda_{ns}a)\right] \tag{23}$$

The laser beam as compared to electron beam may be considered to be a sum of decoupled transverse modes, and one can write using a superposition of different transverse modes:

$$I = \sum_{i,\,m,\,n} p_i I_{mn} \tag{24}$$

where p_i are real numbers chosen in such a way to obtain the wanted laser intensity (from spatial distribution and intensity values' point of view).

3. Simulations and comments

Let us consider the cladding processing on a Cu substrate. The input parameters corresponding to **Figures 1–7** are collected in **Table 1**. We have chosen various

situations, for example, different transverse modes (for laser beam), various velocities, incident powers and values of H.

For electron beam processing [7], one may consult the Katz and Penfolds absorption law [8] and also Tabata-Ito-Okabe absorption law [9].

In **Figure 1**, the thermal field for Gaussian laser beam is presented, when V = 0 mm/s, P = 1 KW, H = 2 mm and the substrate is Cu. In **Figure 2** the thermal field for Gaussian laser beam is given when V = 10 mm/s, P = 1 KW and H = 2 mm. In **Figure 3** the thermal field for TEM_{03} laser beam is presented, when V = 0 mm/s, P = 2 KW and H = 3 mm. **Figure 4** shows the thermal field for TEM_{03} laser beam, when V = 10 mm/s, P = 4 KW and H = 4 mm. **Figure 5** represents the thermal field for TEM_{03} laser beam, when V = 100 mm/s, P = 10 KW and H = 3 mm.

If one compares **Figures 1** and **2**, the differences in the spatial distribution of thermal field for the two cases can be seen. On the other hand, the comparison of **Figures 3–5** shows that for TEM_{03} we do not have significant changes in thermal profile but a proportional increase of the incident power with H.

In **Figures 6** and **7**, we have as scanning source an electron beam of power P = 1 KW. If in **Figure 6** V = 0 mm/s, while in **Figure 7** the speed is V = 10 mm/s. Our simulations show a decrease of thermal field with the increase of scanning velocity.

As observed from **Table 2**, Cu behaves very similarly with Au, Ag and Al from a thermal point of view [10]. Accordingly, we may consider that **Figures 1–7** are also meaningful if we use substrates from Au, Ag or Al.

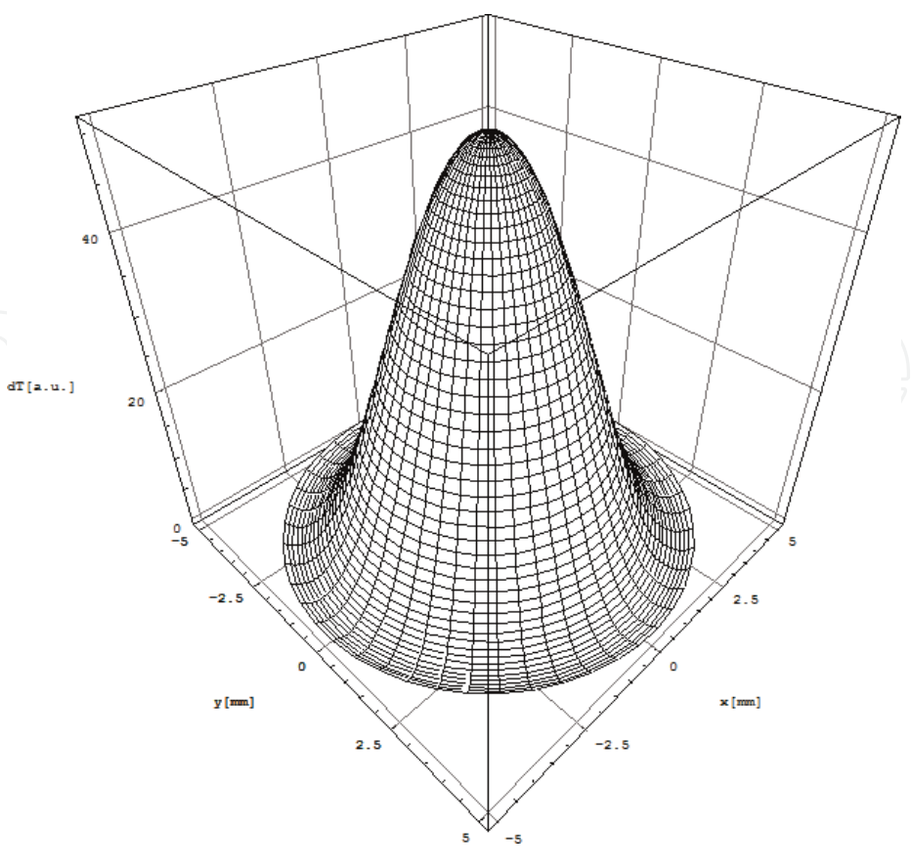

Figure 1.
The thermal field for a Gaussian laser beam when V = 0 mm/s, P = 1 KW and H = 2 mm. The substrate is supposed to be from Cu.

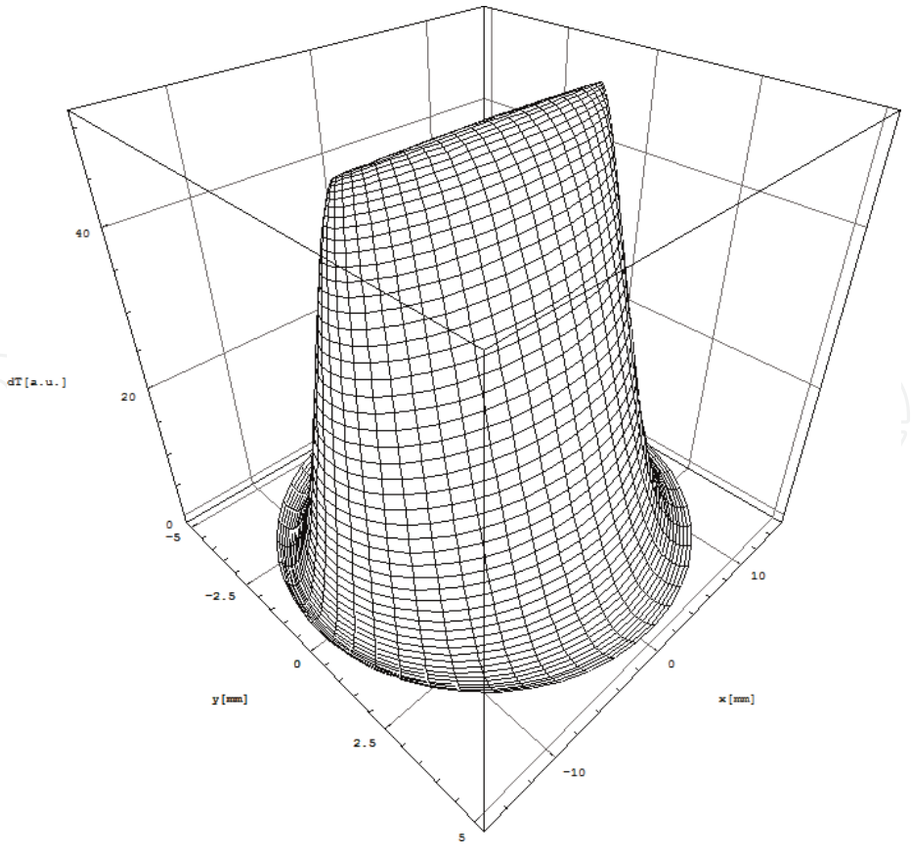

Figure 2.
The thermal field for a Gaussian laser beam when V = 10 mm/s, P = 1 KW and H = 2 mm. The substrate is supposed to be from Cu.

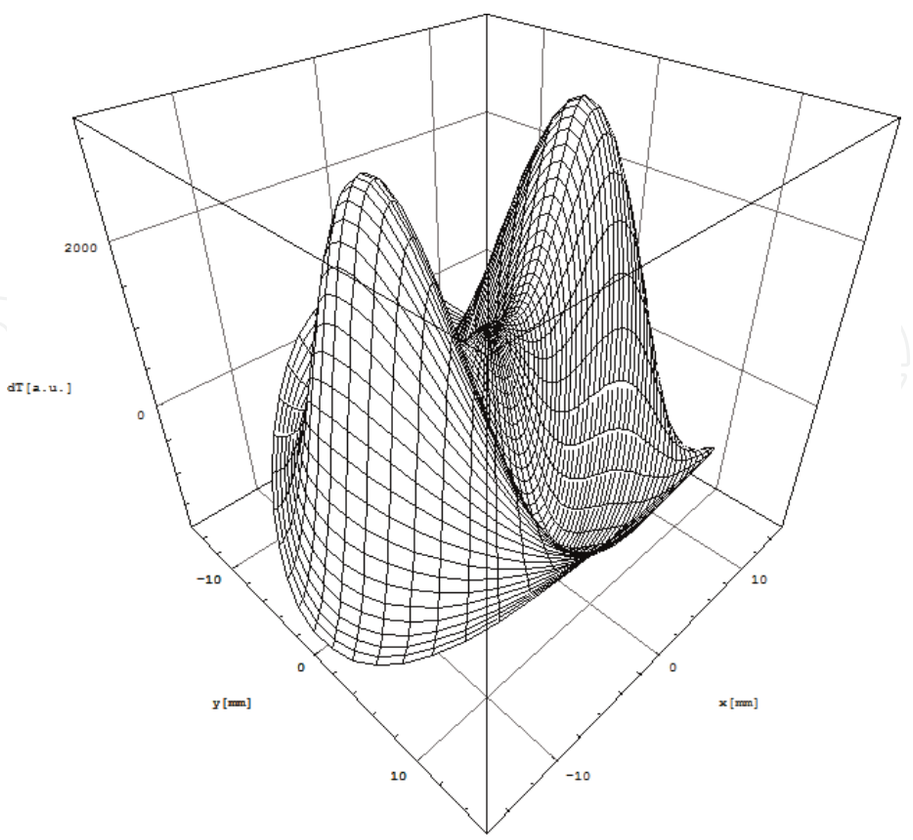

Figure 3.
The thermal field for a TEM_{03} laser beam when V = 0 mm/s, P = 2 KW and H = 3 mm. The substrate is supposed to be from Cu.

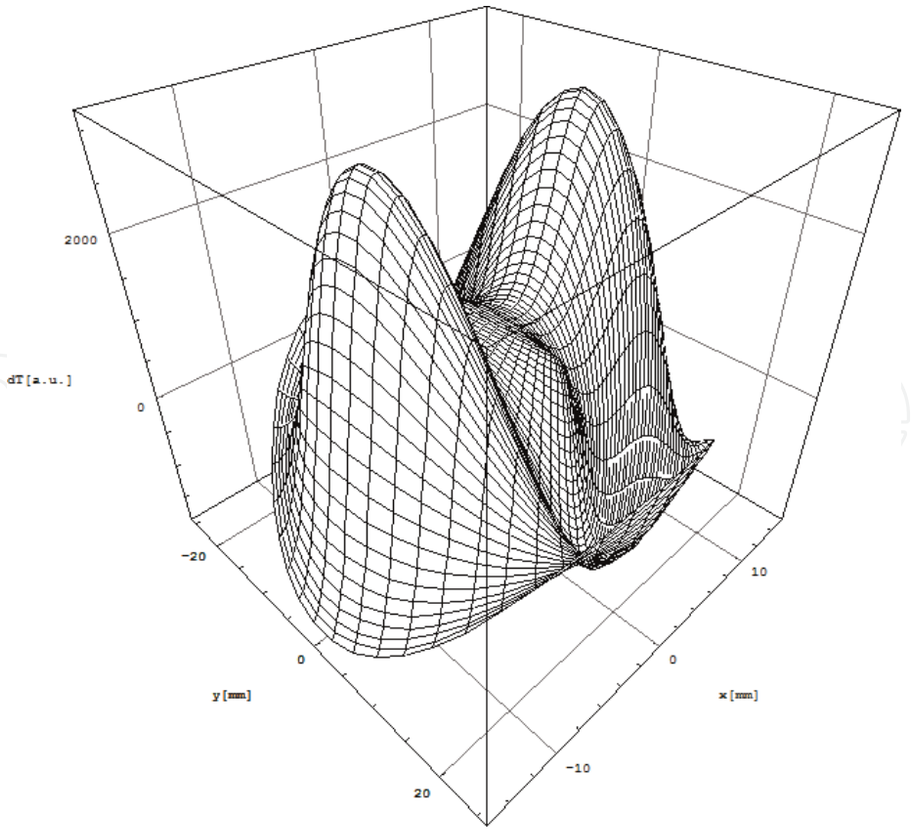

Figure 4.
The thermal field for a TEM_{03} laser beam when V = 10 mm/s, P = 4 KW and H = 4 mm. The substrate is supposed to be from Cu.

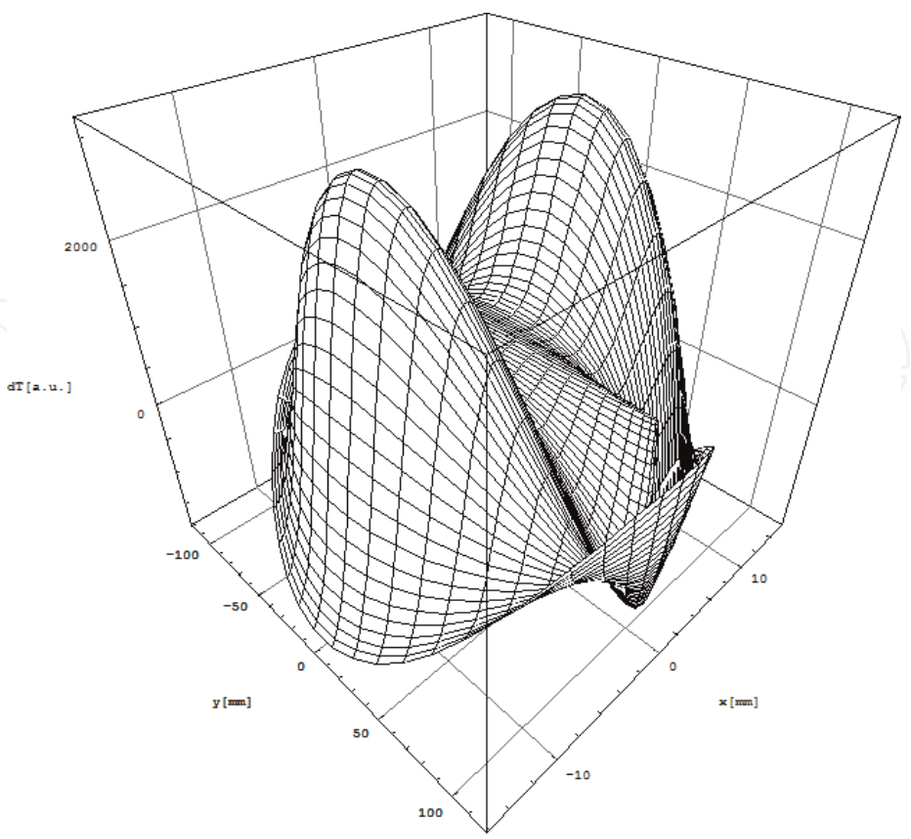

Figure 5.
The thermal field for a TEM_{03} laser beam, when V = 100 mm/s, P = 10 KW and H = 3 mm. The substrate is supposed to be from Cu.

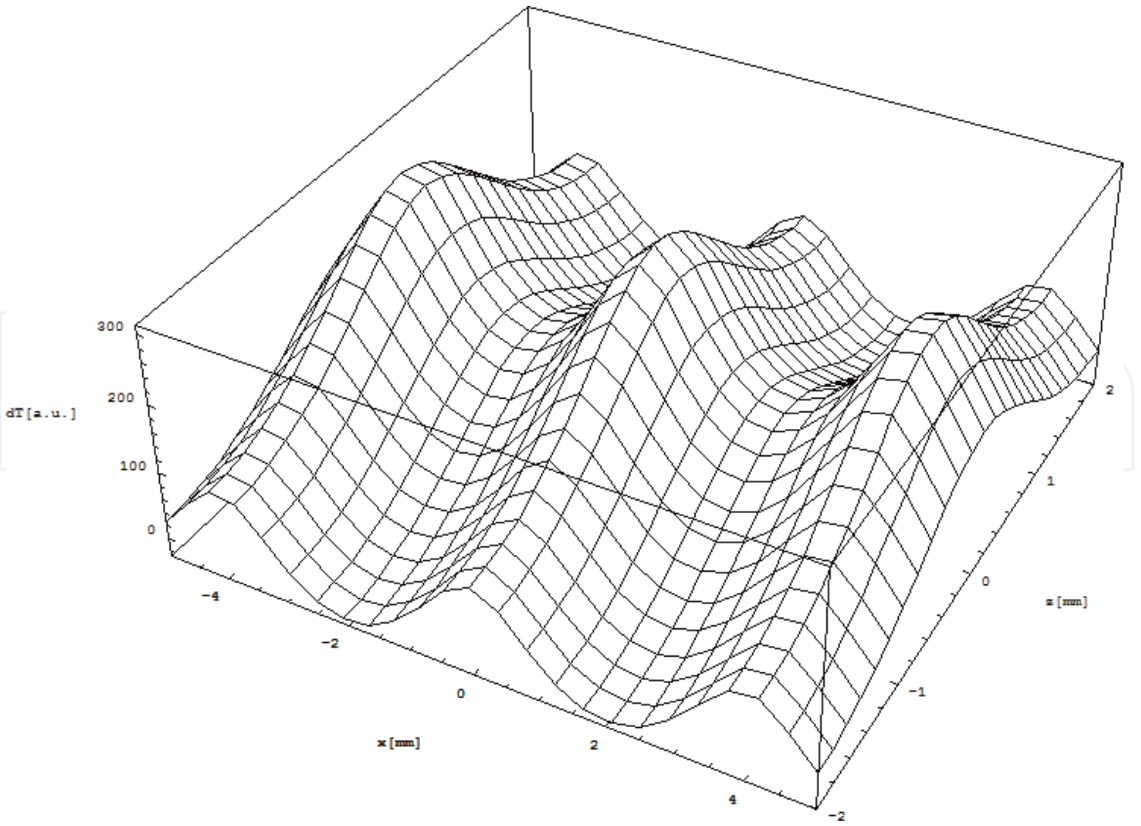

Figure 6.
The thermal field for a Gaussian electron beam when V = 0 mm/s, P = 1 KW and H = 2 mm. The substrate is supposed to be from Cu.

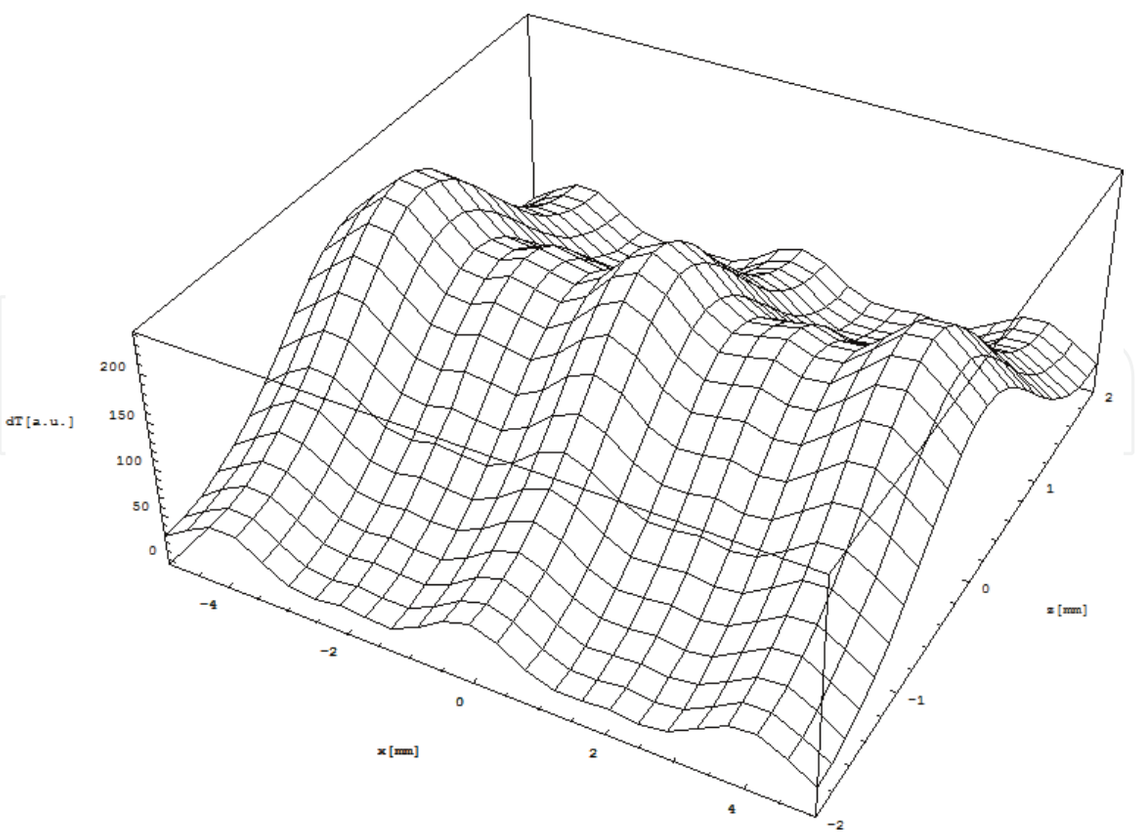

Figure 7.
The thermal field for a Gaussian electron beam when V = 10 mm/s, P = 1 KW and H = 2 mm. The substrate is supposed to be from Cu.

Figure no.	Beam type	Mode	Velocity [mm/s]	Incident power [kW]	Melted pool depth H [mm]	Thermal diffusivity γ [cm^2/s]	Thermal conductivity k [W/cmK]
Figure 1	Laser	TEM_{00}	0	1	2	1.14	3.95
Figure 2	Laser	TEM_{00}	10	1	2	1.14	3.95
Figure 3	Laser	TEM_{03}	0	2	3	1.14	3.95
Figure 4	Laser	TEM_{03}	10	4	4	1.14	3.95
Figure 5	Laser	TEM_{03}	100	10	3	1.14]	3.95
Figure 6	Electron	TEM_{00}	0	1	2	1.14	3.95
Figure 7	Electron	TEM_{00}	10	1	2	1.14	3.95

Table 1.
*The input parameters for the **Figures 1–7**.*

Element	Thermal diffusivity γ [cm^2/s]	Thermal conductivity k [W/cmK]
Cu	1.14	3.95
Au	1.22	3.15
Ag	1.72	4.28
Al	1.03	2.4

Table 2.
The thermal parameters for: Cu, Au, Ag and Al.

4. Conclusions

Our major conclusions are as follows: apart from Gaussian case, the increase in velocity of the other transversal modes does not affect too much the thermal profile; and second the large difference between the electron cladding and laser cladding is that in electron cladding an increase of beam velocity affects in an important amount the values of the thermal fields. The higher the velocity of electron beam, the lower the thermal fields at the surface sample. Our major conclusions are in good agreement with experimental data from literature; see, for example, references [11, 12]. On the other hand, it is known that there are some limitations in laser cladding, for example, high initial capital cost, high maintenance cost and presence of heat affected zone. For electron cladding, one can conclude that the cost is reduced as there are no involved mechanical cutting force, work holding and fixturing.

Acknowledgements

The authors acknowledge the support of MCI-OI under the contract POC G 135/2016.

Conflict of interest

The authors declare no conflict of interest.

Author details

Mihai Oane[1], Ion N. Mihăilescu[2] and Carmen-Georgeta Ristoscu[2*]

1 Electrons Accelerators Laboratory, National Institute for Lasers, Plasma and Radiation Physics, Măgurele-Ilfov, Romania

2 Lasers Department, National Institute for Lasers, Plasma and Radiation Physics, Măgurele-Ilfov, Romania

*Address all correspondence to: carmen.ristoscu@inflpr.ro

References

[1] Oane M, Ticos D, Ticoş CM. Charged Particle Beams Processing Versus Laser Processing. Germany: Scholars' Press; 2015. pp. 60-61, ISBN: 978-3-639-66753-0, monograph

[2] Oane M, Peled A, Medianu RV. Notes on Laser Processing. Germany: Lambert Academic Publishing; 2013. pp. 7-9, ISBN: 978-3-659-487-48739-2, monograph

[3] Oane M, Medianu RV, Bucă A. Chapter 16: A parallel between laser irradiation and electrons irradiation of solids. In: Radiation Effects in Materials. IntechOpen; 2016. pp. 413-430, ISBN: 978-953-51-2417-7, monograph

[4] Steen WM, Mazumder J. Laser Material Processing. London, Dordrecht, Heidelberg, New York: Springer; 2010, ISBN: 978-1-84996-061-8, monograph

[5] Cline HE, Anthony TR. Heat treating and melting material with a scanning laser or electron beam. Journal of Applied Physics. 1977;**48**(9):3895-3900. DOI: 10.1063/1.324261

[6] Picasso M, Marsden CF, Wagniere JD, Frenk A, Rappaz M. A simple but realistic model for laser cladding. Metallurgical and Materials Transactions B. 1994;**25**(B):281-291. DOI: 10.1007/BF02665211

[7] Mul D, Krivezhenko D, Zimoglyadova T, Popelyukh A, Lazurenko D, Shevtsova L. Surface hardening of steel by electron-beam cladding of Ti+C and Ti+B_4C powder compositions at air atmosphere. Applied Mechanics and Materials. 2015;**788**: 241-245. DOI: 10.4028/www.scientific.net/AMM.788.241

[8] Oane M, Toader D, Iacob N, Ticos CM. Thermal phenomena induced in a small graphite sample during irradiation with a few MeV electron beam: Experiment versus theoretical simulations. Nuclear Instruments and Methods in Physics Research B. 2014; **318**:232-236. DOI: 10.1016/j.nimb.2013.09.017

[9] Oane M, Toader D, Iacob N, Ticos CM. Thermal phenomena induced in a small tungsten sample during irradiation with a few MeV electron beam: Experiment versus simulations. Nuclear Instruments and Methods in Physics Research B. 2014;**337**:17-20. DOI: 10.1016/j.nimb.2014.07.012

[10] Bauerle D. Laser Processing and Chemistry. 2nd ed. Berlin: Springer; 1996; ISBN 10: 354060541X/ISBN 13: 9783540605416

[11] Wirth F, Eisenbarth D, Wegener K. Absorptivity measurements and heat source modeling to simulate laser cladding. Physics Procedia. 2016;**83**: 1424-1434. DOI: 10.1016/j.phpro.2016.08.148

[12] Meriaudeau F, Truchetet F, Grevey D, Vannes AB. Laser cladding process and image processing. Journal of Lasers in Engineering. 1997;**6**:161-187